An analysis of flooding coverage using remote sensing within the context of risk assessment

Tatiana Solovey

Polish Geological Institute – National Research Institute, Department of Hydrogeology and Environmental Geology,
Rakowiecka 4, 00-975 Warsaw, Poland
*e-mail: tatiana.solovey@pgi.gov.pl

Abstract

Results of research of the identification of flooding as a result of groundwater table fluctuations on the example of the valley of the River Vistula, with the use of multi-spectral Sentinel-2 images from the years 2017–2018 are presented. An analysis of indexes of water use, calculated on the basis of green, red and shortwave infrared (SWIR) bands, for extraction of water objects and flooded areas was carried out. Based on the analyses conducted, a mapping method was developed, using three water indexes (MNDWI Modified Normalised Difference Water Index, NDTI Normalised Difference Index and NDPI Normalised Difference Pond Index). Results show that the 10 metre false colour composite $R_{NDTI}G_{NDPI}B_{MNDWI}$ obtained significantly improved submerged extractions more than did individual water indexes. Moreover, the 10-m-images of MNDWI and NDPI, obtained by the sharpening High Pass Filter (HPF), may represent more detailed spatial information on floods than the 20-m-MNDWI and NDPI, obtained from original images.

Key words: Sentinel-2, Remote Sensing, flood mapping, Water Indexes

1. Introduction

The Flood Directive 2007/60/EC addresses issues of inclusion of groundwater-related flooding on maps of threats and risks. Flooding caused by high levels of groundwater table does not have a precise definition, nor assessment principles, in current Polish legislation. The first comprehensive work on a national scale is that of a methodology for the preparation of preliminary flood risk assessment (WORP), for groundwater-related flooding (Janica et al., 2017). This defines the method of identifying areas exposed to two basic types of flooding (i.e., from groundwater and runoff) and conducting preliminary flood risk assessment. The use of the remote sensing method was recommended in order to identify areas with frequencies high water levels at the surface.

The present paper attempts to determine the optimal method of analysing the extent of flooding by remote sensing for the purpose of assessing the risk of groundwater-related flooding. The main assumption is the use of free satellite observation data and an efficient and of an easy-to-use automatic method of mapping the extent of flooding.

MODIS, Landsat and, currently, Sentinel satellite images are the most widely used in the monitoring of the natural environment. MODIS data have a low spatial resolution and a high time resolution; on their basis, flooded wetlands cannot be accurately determined and smaller objects cannot be identified, while images with a better spatial resolution, such as Landsat data, always have a low time frequency. The European Space Agency (ESA) has made great progress in increasing the efficiency of the mapping of flooded areas and water bodies by introducing a

new precise, optical spatial resolution using the Sentinel-2 satellite. Certainly, Sentinel-2 images have a great potential for flood mapping on a regional scale, on account of its attractive properties (i.e., spatial resolution of 10 metres for four bands and a 10-day return frequency) and free access.

In the mapping of flooded areas and water bodies, remote sensing methods based on analysis of single band density slicing (Butera, 1983; Martinez & Le Toan, 2007; Melack & Hess, 2010; Morandeira et al., 2016; Moser et al., 2016), unsupervised and supervised classification (Ramsey & Laine, 1997; Zomer et al., 2009; Mwita et al., 2013; Huang et al., 2014a; Napiórkowska, 2014; White et al., 2015) and spectral water indexes (Li & Chen, 2005; Huang et al., 2014b; Li et al., 2016; Nandi et al., 2017) are currently used. The flooded mapping method based on spectral water indexes is currently very popular, because it is easy to apply, efficient and has low computing costs. The most useful spectral water indexes for wetland classification are the Normalised Difference Vegetation Index (NDVI) (Kayastha et al., 2012), Land Surface Water Index (LSWI) (Dong et al., 2014), Normalised Difference Water Index (NDWI) (McFeeters, 1996; Seiler et al., 2009; Dvorett et al., 2016), Modified Normalised Difference Water Index (MNDWI) (Xu, 2006) and a Soil and Atmosphere Resistant Vegetation Index (SARVI) (Huete et al., 1997).

A combination of three spectral water indexes was used to identify floodplain and water bodies: the Modified Normalised Difference Water Index (MNDWI), Normalised Difference Pond Index (NDPI) and Normalised Difference Turbidity Index (NDTI). A combination of these indexes strengthens the range of water reservoirs, water and swamp vegetation and water turbidity, which makes it easy to identify wetlands.

The aim of the present study is twofold; to assess the usefulness of created 10-m-composite images of the water indexes MNDWI, NDPI and NDTI, based on Sentinel-2 images for the years 2017–1018, in the mapping of flooding in the test area and to define the method of applying the method of flood mapping proposed for the development of maps of areas threatened by flooding.

2. Material and methods

The study area is situated in the central part of the valley of the River Vistula in Poland, part of which is located in the Kampinos National Park (KNP), which is also a Natura 2000 area and has an areal extent of 385 km^2 (Fig. 1). The KNP is in the central Mazovian Lowland in the valley of the River Vistula, northwest of Warsaw.
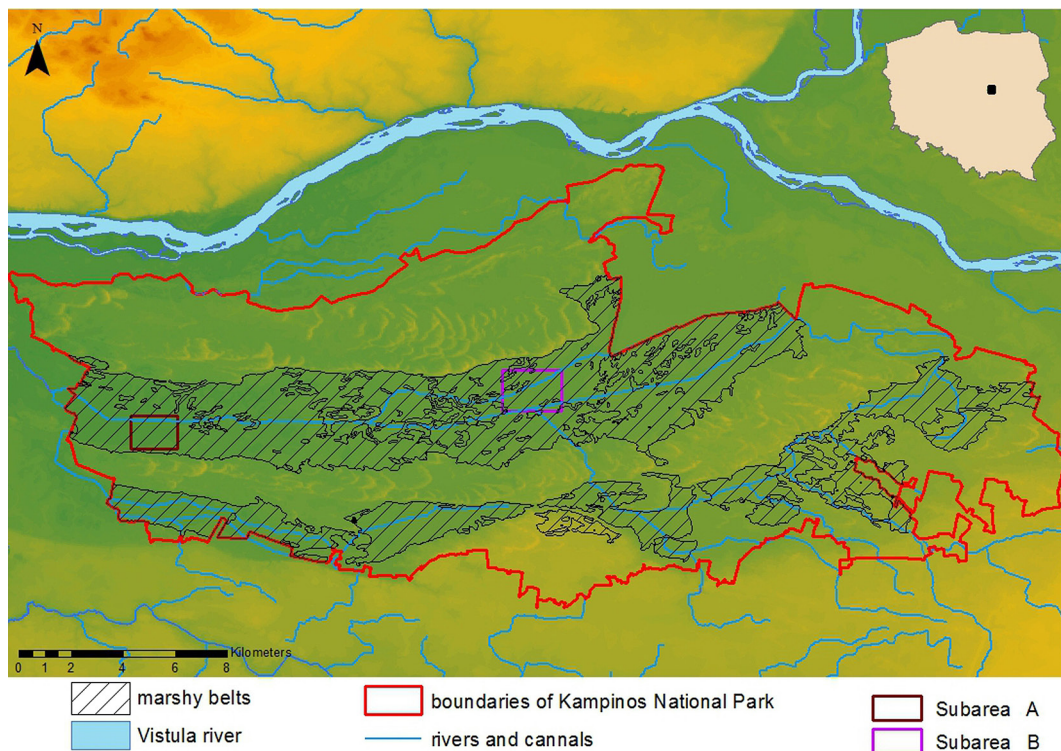

Fig. 1. Location of the study area on the background of DTM

The average ordinates of the KNP area, which is substantially even, is about 80 metres above sea level (Krogulec, 2004). The landscape is characterised by a latitudinal belt of dunes. From the north extends the flood terrace of the River Vistula. Further to the south runs the terrace of the Kampinos Forest, which consists of two alternating dune and marshy strips and the terrace of the Łowicko-Błońska Plain (Krogulec, 2011). The climate is moderate with an average annual temperature over a longer period (1994 to 2016) of 8.7°C and an average annual precipitation of 568.1 mm (Olszewski et al., 2018).

The valuable natural wetlands are the basic ecosystem for which the KNP was established covering 176.9 km^2 (Kopeć et al., 2013). The northern swamp belt, with an area of about 10,000 ha, is much better developed than the southern one, swamps having been turned into meadows and pastures. The southern swamp belt, with an area of approximately 7,000 ha, is fragmented into several valleys that no longer form a distinct belt. Wet meadows and sedges prevail in this belt (Michalska-Hejduk, 2001).

The dataset used in the present study is the Sentinel-2 Level 1C product in the UTM/WGS84 projection, which was downloaded from the ESA Sentinel-2 Pre-Operations Hub (https://scihub.copernicus.eu/). A subset covering 40 × 17 km and cantered at 52°24'35"N, 20°17'3"E was used for the case study. For the analysis, Sentinel-2 image was used with a zero cloud in 2017–2018. The date of acquisition is presented in Table 1.

The Modified Normalised Difference Water Index (MNDWI) (Xu, 2006) is defined as:

$$\text{MNDWI} = \frac{\rho_{Green} - \rho_{SWIR}}{\rho_{Green} + \rho_{SWIR}} \qquad (1)$$

where ρ_{Green} is the TOA reflectance value of the green band and ρ_{SWIR} is the TOA reflectance value of the SWIR band 11. Comparing to the raw Digital Numbers (DN), TOA reflectance is more suitable in calculating MNDWI (Li et al., 2013). The freely available Sentinel-2 Level-1C dataset is already a standard product of TOA reflectance (Drusch et al., 2012).

Compared to NDWI (Gao, 1996), water bodies have greater positive values in MNDWI, because water bodies absorb more SWIR light than NIR light; soil, vegetation and built-up classes have smaller negative values, because they reflect more SWIR light than green light (Sun et al., 2012).

For Sentinel-2, the green band has a spatial resolution of 10 metres, while the SWIR band (Band 11) has a spatial resolution of 20 metres. Thus, MNDWI needs to be calculated at a spatial resolution of either 10 or 20 metres. In the present study, the spatial resolution of the SWIR band was increased from 20 to 10 metres by using pan-sharpening algorithms. For this purpose, the High Pass Filter (HPF) has been selected (Chavez et al., 1991), because HPF produces a sharpened 10-m-SWIR band with a higher resolution.

The classic NDVI did not work well in the case of vegetation in floodplains with a shallow body of water, which is why the NDPI was developed.

The Normalised Difference Pond Index (NDPI) (Lacaux et. al., 2007) is defined as:

$$\text{NDPI} = \frac{\rho_{Green} - \rho_{SWIR}}{\rho_{Green} + \rho_{SWIR}} \qquad (2)$$

where ρ_{SWIR} is the TOA reflectance value of the SWIR band 12 and ρ_{Green} is the TOA reflectance value of the green band.

As in the case of MNDWI, for the NDPI calculation, the spatial resolution of the SWIR band Sentinel-2 should be increased from 20 to 10 metres by using pan-sharpening algorithms based on the High Pass Filter (HPF).

Normalised Difference Turbidity Index (NDTI) (Lacaux et al., 2007), which effectively captures turbid water reservoirs that were often confused with open soil on remote sensing images, because an increase in water turbidity and associated radiometric response causes the turbid water reservoirs to behave like open soils (Guyot, 1989). The NDTI indicator uses green and red bands of images from the remote sensing based on the phenomenon that the level of water turbidity increases due to the increase of particles suspended in water, which caus-

Table 1. Summary of remotely sensed datasets used for the present study

Sensor name	Sensor type	Acquisition date	Band information	Resolution (m)
Sentinel-2	Optical	29/03/2017	Blue (490 nm)	10
		2/10/2017	Green (560 nm)	10
		26/12/2017	Red (665 nm)	10
		8/01/2018	NIR (842 nm)	10
		19/03/2018	SWIR (1610 nm)	20
			SWIR (2190 nm)	20

es a greater reflection of the red band than the green (Islam & Sado, 2006).

The Normalised Difference Turbidity Index (NDTI) (Lacaux et. al., 2007) is defined as:

$$\text{NDTI} = \frac{\rho_{Red} - \rho_{Green}}{\rho_{Red} + \rho_{Green}} \tag{3}$$

where ρ_{Red} is the TOA reflectance value of the red band and ρ_{Green} is the TOA reflectance value of the green band.

The analysis was divided into three main stages:
1. Automatic detection of flood extent using image threshold segmentation based on threshold values for MNDWI, NDPI and NDTI.
2. Semi-automatic detection of the extent of flooding using the classification supervised by the colour composite of Red (NDTI) – Blue (MNDWI) – Green (NDPI).
3. Validation of flooded and water bodies maps based on coefficient Kappa. Monserud & Leemans (1992) suggested that values Kappa coefficient lower than 0.4 represent poor or very poor agreement, values from 0.4 to 0.55 represent fair agreement, values from 0.55 to 0.7 represent good agreement, values from 0.7 to 0.85 represent very good agreement and values higher than 0.85 represent an excellent agreement between images.

3. Results

The analysis was carried on archive satellite data for the years 2017–2018 (Table 1). For each acqui-
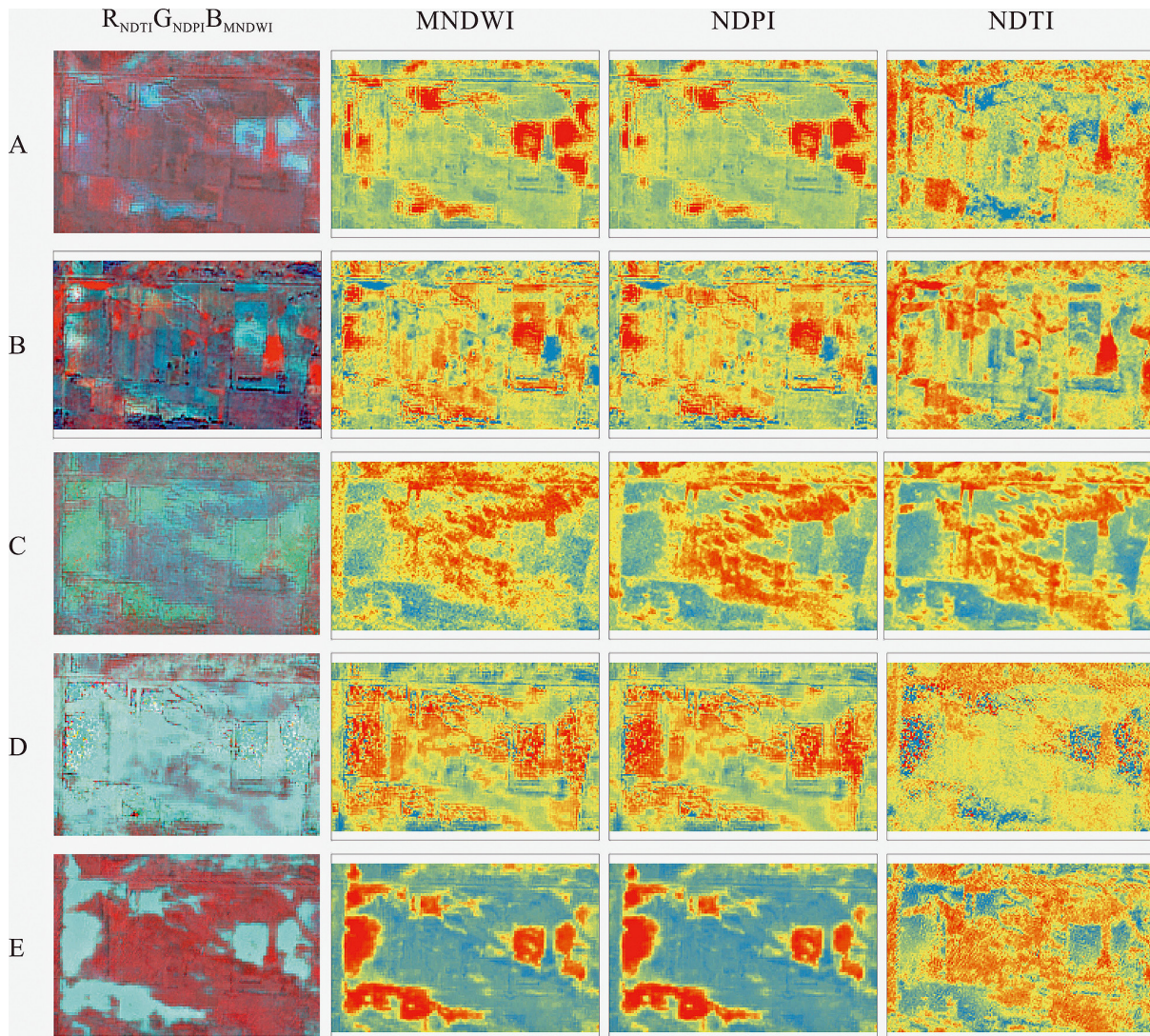

Fig. 2. Subarea A of the 10-m-false colour composite $R_{NDTI}G_{NDPI}B_{MNDWI}$, MNDWI, NDPI and NDTI images for acquisition dates: **A** – March 29, 2017; **B** – October 2, 2017; **C** – December 26, 2017; **D** – January 8, 2018; **E** – March 19, 2018. Surface water is blue on images $R_{NDTI}G_{NDPI}B_{MNDWI}$ and red on images MNDWI, NDPI and NDTI

sition date for subareas A and B, four water index images were developed, $R_{NDTI}G_{NDPI}B_{MNDWI}$, MNDWI, NDPI and NDTI, as shown in Figure 2. Results of the detection of flooded areas and water bodies in the images have been compared.

Compared to areas flooded with a translucent vegetation cover, water reservoirs are the easiest to identify. Accurate mapping of water reservoirs is possible on the basis of threshold image segmentation by the automatic method.

An automatic approach to the detection of water reservoirs is to define a threshold value for mapping of water MNDWI images, NDPI and NDTI. For this purpose, appropriate training fields for the mapping of water surfaces were selected for each acquisition date. In order to verify the correctness of the selected testing fields for separating water bodies from background features, the spectral distance method according to Jeffreys-Matusit (Jensen, 1996) was used. The threshold for the maximum spectral distance JMab equal to 2 was used, indicating complete class separation.

Table 2 contains a list of statistical parameters of training fields for water body with reference to water indexes – MNDWI, NDTI, NDPI.

The MNDWI indicator provides the greatest distinguishability of water body compared to NDPI and NDTI. Poor suitability for identification of water body is indicated by the NDTI index, because the water mapping values (from -0.03 to 0.03) are mostly similar to those of arable land with a vegetation cover. Therefore, threshold values for the water mapping were determined for MNDWI images. The optimal final value was calculated by the OTSU algorithm (Lin, 2005). Due to the significant time diversity of the threshold (from 0.15 to 0.47), a multi-threshold method of image segmentation was used.

The next stage was related to the performance of a pixel classification supervised using the combination of water indexes as false colour composite $R_{NDTI}G_{NDPI}B_{MNDWI}$ and testing fields for flooded with a translucent plant cover. The classification was made using the maximum likelihood method in the Erdas Imagine environment. The definition of flooding in forest areas was abandoned due to the inability to define this class clearly on the basis of the applied $R_{NDTI}G_{NDPI}B_{MNDWI}$ composition.

Overall Accuracy OA and Kappa indicators were used to quantify the accuracy of flooded maps of regions A and B. Table 3 illustrates the high level of recognition of non-forest flooded areas. The Kappa coefficient shows quite stable and high values. The average values of the Kappa coefficient are

Table 2. Maximum (Max), minimum (Min), mean and standard deviation (SD) values of water body within MNDWI, NDTI and NDPI

Acquisition date	Water indexes	Min	Max	Mean	SD	Number of training areas	Threshold
29/03/2017	MNDWI	0.44	0.77	0.65	0.06		0.47
	NDPI	0.39	0.74	0.61	0.07	103	–
	NDTI	−0.04	0.04	0.00	0.02		–
2/10/2017	MNDWI	−0.37	0.81	0.25	0.24		0.15
	NDPI	−0.48	0.77	0.10	0.25	80	–
	NDTI	−0.36	0.14	−0.18	0.13		–
26/12/2017	MNDWI	0.12	0.40	0.24	0.05		0.28
	NDPI	0.13	0.39	0.25	0.06	80	–
	NDTI	−0.11	0.13	0.01	0.05		–
8/01/2018	MNDWI	0.40	0.92	0.64	0.14		0.33
	NDPI	0.27	0.98	0.58	0.14	73	–
	NDTI	−0.49	0.03	−0.18	0.11		–
19/03/2018	MNDWI	0.42	0.64	0.53	0.05		0.41
	NDPI	0.36	0.59	0.48	0.05	80	–
	NDTI	−0.04	0.03	0.00	0.01		–

Table 3. Kappa and Overall Accuracy (OA) of resulting flood maps in subareas A and B

Accuracy indicators		Acquisition date				
		29/03/2017	2/10/2017	26/12/2017	8/01/2018	19/03/2018
Kappa	A	0.8700	0.8334	0.8905	0.8579	0.8971
	B	0.8954	0.8289	0.8828	0.8756	0.9070
OA	A	97.61%	97.13%	94.67%	93.12%	94.99%
	B	94.91%	94.28%	96.02%	97.78%	96.79%

0.86978 – for area A and 0.87794 – for area B. The greatest errors are obtained in the period of active biomass development, exemplified by October 2, 2017. It is not possible to catch water on the surface in highly vegetated areas, consisting of larger-sized plant taxa (e.g., *Phragmition* and *Magnocaricion*).

4. Discussion

The proposed two-level method of identifying floodings can be effectively used on account of the satisfactory accuracy and automatic mapping in the assessment of flood risk (WORP) in the field of groundwater-related flooding. The advantage of this approach is the separate extraction of water reservoirs and areas flooded with water with a translucent vegetation cover, which ensures the distinction between flooded areas and water reservoirs. In the proposed approach, the effectiveness of mapping depends on two factors, i.e., the correctness of choosing the threshold value for water mapping and the proper selection of acquisition scenarios.

When selecting the threshold for water mapping, so as to avoid subjective judgement, the segmentation method of the Otsu threshold was used. However, in the case of regional mapping of large-scale flooding in the context of risk assessment, one threshold is not sufficient to extract water from the background due to the spatially differentiated spectral contrast. Therefore, a multi-threshold method of image segmentation is required when applying regional mapping.

Another important factor is the selection of such acquisition dates that will enable the capture of floods caused by the occurrence of groundwater table raised above the surface. It is recommended to compare satellite images for periods of hydrogeological highs and droughts in order to isolate periodic floods occurring only during wet periods. Flooding from groundwater is a periodic wetness in the area of shallow occurrence (up to depths of 2 metres) of the groundwater table. In other cases, flooding is caused by unfavorable geological, morphological and anthropogenic conditions. They generate runoff water due to the difficult surface runoff and low absorption of the aeration zone.

5. Conclusions

Flood risk assessment from groundwater provides the identification of areas with high frequency of water occurrence on the surface outside the floodplain. Research should use remote sensing methods offered by modern satellite technology, enabling comprehensive, repeatable measurements, carried out simultaneously on large areas, often difficult to access. The newly introduced Sentinel-2 system provides high resolution multispectral images and a satisfactory time resolution, thereby producing an important dataset for mapping of floods. The suggested method of mapping floods on the Sentinel-2 subset by creating a 10-metre MNDWI, NDPI and NDTI images allows to capture not only areas completely flooded, but also wetlands with a low vegetation cover.

The experiment from the Kampinos National Park in Poland shows that the combination of water indicators MNDWI, NDPI and NDTI is more effective in improving the recognition of flooding and distinguishing this from water bodies. The idea of the proposed connection lies in the mutual complementation of spectral water indexes in the recognition of flooding. While the MNDWI indicator best identifies open water, NDPI – captures vegetation in wetlands and water, NDTI – reduces the impact of open soils leading to confusion with turbid water reservoirs. As a result, features are created that more easily distinguish between flooded areas and water bodies.

Acknowledgements

References

Butera, M.K., 1983. Remote sensing of wetlands. *IEEE Transactions on Geoscience and Remote Sensing* 3, 383–392.

Chavez, P.S., Sides, S.C. & Anderson, J.A., 1991. Comparison of 3 different methods to merge multiresolution and multispectral data-Landsat tm and spot panchromatic. *Photogrammetric Engineering and Remote Sensing* 57, 295–303.

Dong, Z.Y., Wang, Z.M., Liu, D.W. & Song, K.S., 2014. Mapping wetland areas using landsat-derived NDVI and LSWI: a case study of west songnen plain, Northeast China. *Journal of the Indian Society of Remote Sensing* 42, 569–576.

Drusch, M., Del Bello, U., Carlier, S., Colin, O., Fernandez, V., Gascon, F., Hoersch, B., Isola, C., Laberinti, P., Martimort, P., Meygret, A., Spoto, F., Sy, O.,

Marchese, F. & Bargellini, P., 2012. Sentinel-2: ESA's optical high-resolution mission for GMES operational services. Remote Sensing of Environment 120, 25–36.

Dvorett, D., Davis, C. & Papes, M., 2016. Mapping and hydrologic attribution of temporary wetlands using recurrent Landsat imagery. *Wetlands* 36, 431–443.

Gao, B.C., 1996. NDWI – A normalized difference water index for remote sensing of vegetation liquid water from space. *Remote Sensing of Environment* 58, 257–266.

Guyot, G., 1989. *Signatures spectrales des surfaces naturelles.* Télédétection satellitaire 5, Paradigme, Caen, 178 pp.

Huang, C., Chen, Y. & Wu, J.P., 2014a. DEM-based modification of pixel-swapping algorithm for enhancing floodplain inundation mapping. *International Journal of Remote Sensing* 35, 365–381.

Huang, C.Q., Peng, Y., Lang, M.G., Yeo, I.Y. & McCarty, G., 2014b. Wetland inundation mapping and change monitoring using Landsat and airborne LiDAR data. *Remote Sensing of Environment* 141, 231–242.

Huete, A., Liu, H., Batchily, K.V. & Van Leeuwen, W., 1997. A comparison of vegetation indices over a global set of TM images for EOS-MODIS. *Remote Sensing of Environment* 59, 440–451.

Islam, M. & Sado, K., 2006. Analyses of ASTER and spectroradiometer data with in situ measurements for turbidity and transparency study of lake Abashri. *International Journal of Geoinformatics* 2, 31–45.

Janica, R., Frankowski, Z., Jóźwiak, K., Kocyła, J., Majer, E., Sokołowska, M., Solovey, T., Woźnicka, M., Honczaruk, M., Kucharska, M. & Majer, K., 2017. *Metodyka opracowania wstępnej oceny ryzyka powodziowego (WORP) w zakresie powodzi od wód podziemnych* [*Methodology for the development of preliminary flood risk assessment (WORP) for flooding from groundwater*]. PIG–PIB, Warszawal, 56 pp.

Jensen, J.R., 1996. *Introductory digital image processing, a remote sensing perspective.* Prentice Hall, 316 pp.

Kayastha, N., Thomas, V., Galbraith, J. & Banskota, A., 2012. Monitoring wetland change using inter-annual Landsat time-series data. *Wetlands* 32, 1149–1162.

Kopeć, D., Michalska-Hejduk, D. & Krogulec, E., 2013. The relationship between vegetation and groundwater levels as an indicator of spontaneous wetland restoration. *Ecolog Engineering* 57, 242–251.

Krogulec, E., 2004. *Ocena podatności wód podziemnych na zanieczyszczenia w dolinie rzecznej na podstawie przesłanek hydrodynamicznych* [*Vulnerability assessment of groundwater pollution in the river valley on the basis of hydrodynamic evidence*]. Uniwersytet Warszawski, Warszawa, 177 pp.

Krogulec, E., 2011. Charakterystyka uwarunkowań hydroekologicznych [Characteristics of hydroecological conditions]. [In:] T. Okruszko, W. Mioduszewski & L. Kucharski (Eds): *Ochrona i renaturyzacja mokradeł Kampinoskiego Parku Narodowego* [*Protection and restoration of wetlands in the Kampinos National Park*]. Szkoła Główna Gospodarstwa Wiejskiego, Warszawa, 73–92.

Lacaux, J.P., Tourre, Y.M., Vignolles, C., Ndione, J.A. & Lafaye, M., 2007. Classification of ponds from highspatial resolution remote sensing: Application to

Rift Valley Fever epidemics in Senegal. *Remote Sensing of Environment* 106, 66–74.

Li, J.H. & Chen, W.J., 2005. A rule-based method for mapping Canada's wetlands using optical, radar and DEM data. *International Journal of Remote Sensing* 26, 5051–5069.

Li, W.B., Du, Z.Q., Ling, F., Zhou, D.B., Wang, H.L., Gui, Y.M., Sun, B.Y. & Zhang, X.M., 2013. A comparison of land surface water mapping using the normalized difference water index from TM, ETM plus and ALI. *Remote Sensing* 5, 5530–5549.

Li, W., Qin, Y., Sun, Y., Huang, H., Ling, F., Tian, L. & Ding, Y., 2016. Estimating the relationship between dam water level and surface water area for the Danjiangkou Reservoir using Landsat remote sensing images. *Remote Sensing Letters* 7, 121–130.

Lin, K.C., 2005. On improvement of the computation speed of Otsu's image thresholding. *Journal of Electronic Imaging* 14, 023011.

Martinez, J. & Le Toan, T., 2007. Mapping of flood dynamics and spatial distribution of vegetation in the Amazon Floodplain using multitemporal SAR data. *Remote Sensing of Environment* 108, 209−223.

McFeeters, S.K., 1996. The use of the normalized difference water index (NDWI) in the delineation of open water features. *International Journal of Remote Sensing* 17, 1425–1432.

Melack, J.M. & Hess, L.L., 2010. *Remote sensing of the distribution and extent of wetlands in the Amazon basin Amazonian floodplain forests*. Springer, pp. 43–59.

Michalska-Hejduk, D., 2001. Stan obecny i kierunki zmian roślinności nieleśnej Kampinoskiego Parku Narodowego [Current state and directions of change of non-forest vegetation of the Kampinos National Park]. *Monographia Botanica* 89, 1–134.

Monserud, R.A. & Leemans, R., 1992. Comparing global vegetation maps with the Kappa statistic. *Ecological Modelling* 62, 275–293.

Morandeira, N.S., Grings, F., Facchinetti, C. & Kandus, P., 2016. Mapping plant functional types in floodplain wetlands: an analysis of C-Band polarimetric SAR data from RADARSAT-2. *Remote Sensing* 8, 174.

Moser, L., Schmitt, A., Wendleder, A. & Roth, A., 2016. Monitoring of the lac Bam wetland extent using dual-polarized X-band SAR data. *Remote Sensing* 8, 302.

Mwita, E., Menz, G., Misana, S., Becker, M., Kisanga, D. & Boehme, B., 2013. Mapping small wetlands of Kenya and Tanzania using remote sensing techniques. *International Journal of Applied Earth Observation and Geoinformation* 21, 173–183.

Nandi, I., Srivastava, P.K. & Shah, K., 2017. Floodplain mapping through support vector machine and optical/infrared images from Landsat 8 OLI/TIRS sensors: case study from Varanasi. *Water Resources Management* 31, 1157–1171.

Napiórkowska, M., 2014. Monitoring wetlands ecosystems using ALOS PALSAR (L-Band, HV) supplemented by optical data: a case study of Biebrza Wetlands in Northeast Poland. *Remote Sensing* 6, 1605–1633.

Olszewski, A., Wierzbicki, A., Degórska, A., Ferchmin, M., Gudowicz, J., Lenartowicz, M. & Otręba, N.,

2018. *Raport stacji bazowej zintegrowanego monitoringu środowiska przyrodniczego „Pożary" za rok 2017* [*Report of the base station of the Integrated Monitoring of Natural Environment „Pożary" for 2017*]. Kampinoski Park Narodowy, Izabelin.

Ramsey, E.W. & Laine, S.C., 1997. Comparison of Landsat thematic mapper and high resolution photography to identify change in complex coastal wetlands. *Journal of Coastal Research* 13, 281–292.

Seiler, R., Schmidt, J., Diallo, O. & Csaplovics, E., 2009. Flood monitoring in a semi-arid environment using spatially high resolution radar and optical data. *Journal of Environmental Management* 90, 2121–2129.

Sun, F.D., Sun, W.X., Chen, J. & Gong, P., 2012. Comparison and improvement of methods for identifying waterbodies in remotely sensed imagery. *International Journal of Remote Sensing* 33, 6854–6875.

White, L., Brisco, B., Dabor, M., Schmitt, A. & Pratt, A., 2015. A collection of SAR methodologies for monitoring wetlands. *Remote Sensing* 7, 7615–7645.

Xu, H.Q., 2006. Modification of normalised difference water index (NDWI) to enhance open water features in remotely sensed imagery. *International Journal of Remote Sensing* 27, 3025–3033.

Zomer, R.J., Trabucco, A. & Ustin, S., 2009. Building spectral libraries for wetlands land cover classification and hyperspectral remote sensing. *Journal of Environmental Management* 90, 2170–2177.